

Research Article

Theme: Team Science and Education for Pharmaceuticals: the NIPTE Model

Guest Editors: Ajaz S. Hussain, Kenneth Morris, and Vadim J. Gurvich

Scale-Up and In-line Monitoring During Continuous Melt Extrusion of an Amorphous Solid Dispersion

Abbe Haser,¹ Brian Haight,² Andreas Berghaus,³ Augie Machado,² Charlie Martin,² and Feng Zhang^{1,4}

Received 26 June 2018; accepted 22 August 2018; published online 25 September 2018

Abstract. Chemical degradation of drug substances remains a major drawback of extrusion. Larger-scale extrusion equipment has advantages over smaller equipment due to deeper flight elements and added flexibility in terms of screw design, unit operations, and residence time. In a previous study, we extruded a meloxicam-copovidone amorphous solid dispersion (ASD) on a Nano-16 extruder and achieved 96.7% purity. The purpose of this study is to introduce a strategy for scaling the process to an extruder with dissimilar geometry and to investigate the impact on the purity of the ASD. The formulation previously optimized on the Nano-16, 10:90 meloxicam and copovidone, was used for scale-up. Our approach to scale-up to the ZSE-18, utilized specific mechanical energy input and degree of fill from the Nano-16. Vacuum was added to prevent hydrolysis of meloxicam. Downstream feeding and micronization of meloxicam were introduced to reduce the residence time. In-line monitoring of the solubilization of meloxicam was monitored with a UV probe positioned at the die. We were able to achieve the same purity of meloxicam with the Micro-18 as we achieved with Nano-16. When process conditions alone were not sufficient, meglumine was added to further stabilize meloxicam. In addition to the chemical stability advantage that meglumine provided, we also observed solubility enhancement which allowed for an increase in drug loading to 20% while maintaining 100% purity.

KEY WORDS: melt extrusion; amorphous solid dispersion; meloxicam; chemical stability; scale-up.

INTRODUCTION

Melt extrusion and spray drying are the two dominant manufacturing technologies for preparing amorphous solid dispersions (ASDs). Melt extrusion allows for continuous manufacturing, does not require organic solvents, and is easily scaled-up [1]. The major drawback of melt extrusion is the thermal exposure to the drug substance. This is most problematic with drug substances that have high melting points (above 200 °C) and therefore require high processing temperatures [2]. This can result in degradation of the drug substance, the polymer carrier, or both. Thermal degradation limits the typical design space of melt extrusion to drug substances with lower melting points [2, 3].

Early development work for extrusion is achieved by using bench-scale extruders such as the Mini Haake® or small-sized extruders such as an 11 or 16 mm screw with an L:D ratio (length

of screw to diameter of screw ratio) of 25:1 or smaller [4]. Optimized formulations developed for clinical phase are typically produced on larger-scale extrusion equipment. Differences can include screw and barrel configurations, free volume, and feed method, all of which can influence the energy input to the system [5]. Another important design variable is melt temperature due to its relationship with degradation and amorphous conversion.

Typically, scaling between equipment cannot be achieved quantitatively; however, there are some general rules that have been applied in the past. The primary strategy, scaling by free volume (V_{free}) [6, 7], relates to scaling within the same geometry or same D_o/D_i ratio (outer to inner screw diameter ratio) [8]. It requires the mass throughput (Q_1) to free volume (V_{free}) to remain constant when moving between extruder equipment. Within the same geometry, V_{free} can be approximated as $V_{\text{free}} \propto D_o^3$ [4], therefore the equation for your new mass throughput (Q_2) is:

$$Q_2 = Q_1 (D_{o,2}/D_{o,1})^{1-3} \quad (1)$$

and for dissimilar geometry:

$$Q_2 = Q_1 (V_{\text{free},2}/V_{\text{free},1})^{1-3} \quad (2)$$

The value of the exponent depends on the process, for instance in a heat transfer limited system, the exponent will be

Guest Editors: Ajaz S. Hussain, Kenneth Morris, and Vadim J. Gurvich

¹ Division of Pharmaceutics, College of Pharmacy, The University of Texas at Austin, 2409 University Avenue, A1920, Austin, Texas 78712, USA.

² Leistritz Extrusion, 169 Meister Ave, Somerville, New Jersey, USA.

³ ColVisTec, Max-Planck-Str. 3, Berlin, Germany.

⁴ To whom correspondence should be addressed. (e-mail: feng.zhang@austin.utexas.edu)

close to 2. Additional considerations include maintaining the L:D ratio, screw design, temperature profile with modification for less barrel contact, screw speed, and die pressure drop. As a result of maintaining these parameters, the specific mechanical energy input (SME), melt temperature at die, degree of fill, and residence time should remain similar. These general rules have been primarily applied for scaling amongst like-geometry equipment and are not directly translatable to small extruders. Limited studies exist in the field of pharmaceuticals that examine scaling among different geometry equipment, specifically scaling from the miniature/small extruders up to pilot-scale extruders [9, 10].

In our previous work, we optimized an extrusion process on a twin-screw co-rotating extruder with a 16-mm diameter [11]. The Nano-16 extruder was designed to keep batch-size small to enable early formulation development and therefore has minimal free volume. Consequently, at the same screw speed, the material inside the extruder is exposed to a relatively higher amount of shear as the depth of the screw elements is much shallower than in the larger extruders with more free volume. In this case, scaling to a larger extruder could offer an advantage by reducing shear and subsequently degradation. Larger equipment also introduces the possibility for additional unit operations which could also be used to reduce degradation or improve the quality of the processed material. Typical unit operations include vacuum capability and increased devolatilization as well as additional temperature control and process flexibility due to additional zones, side-stuffing or downstream feedings, and injection ports. Even with the potential for improved material processing, there are still some considerations that should be made when scaling to larger equipment. Despite the advantage of a larger overflight gap, which when maintained at the same screw speed as the smaller extruders results in less shear, venting, devolatilization, and heat transfer can become more challenging as the process is scaled-up.

The purpose of this study was to propose a strategy for scaling an optimized process between equipment with dissimilar geometries and additionally investigate any advantages that scaling the process might have in terms of chemical degradation for a thermally labile and high melting compound. Due to the lack of examples from the pharmaceutical field, principles from the plastic industry were applied [6, 12]. The ASD system, 10:90 meloxicam, and copovidone, from our previous work was chosen as the model system [11]. In that previous study, a formulation alteration was required to completely stabilize meloxicam. A base, meglumine, was added to disrupt the degradation pathway of meloxicam. Meglumine was also necessary on the larger scale to chemically stabilize meloxicam.

MATERIALS AND METHODS

Materials

BASF Corporation (Florham Park, NJ) kindly donated Kollidon® VA 64 (PVPVA), a vinylpyrrolidone–vinylacetate copolymer with a weight average molecular weight of 65,000 g/mol. ShenZhen Nexconn Pharmatechs Ltd. (ShenZhen, China) supplied the meloxicam. Meglumine was purchased from EMD Millipore Corp. (Billerica, MA). High-performance liquid chromatography (HPLC)-grade acetonitrile was purchased from Fisher Scientific (Pittsburgh, PA). All other chemicals were of ACS grade or higher.

Melt Extrusion

Copovidone was dried at 70 °C for a minimum of 4 h before extrusion studies to reduce moisture. A physical blend consisting of 10% (w/w) meloxicam and 90% (w/w) copovidone was prepared by geometric dilution and subsequently mixed in a 16.0-ft³ Twin Shell Dry Blender (V-Blender) (Patterson-Kelly, East Stroudsburg, PA) for 10 min. Four different extrusion studies were completed to scale the process. Experiments were performed on a Leistritz ZSE Micro-18 co-rotating twin screw extruder (Leistritz Extrusion, Somerville, New Jersey) equipped with a 3-mm round die. A gravimetric feeder (Brabender Technologie, Ontario, Canada) was used to accurately feed the extruders. A 600-mbar vacuum was pulled when necessary to remove moisture. The feeding zone was maintained at room temperature conditions with water circulation. The melt temperature and torque were recorded and monitored for all conditions. Following all extrusion studies, the rods of extrudate were milled using an impact mill (Intertek, Springfield, NJ) and passed thru a 70-mesh (210 μm) sieve prior to any characterization.

Scale-Up

The design considerations from the optimized extrusion process on the Nano-16 extruder equipment were considered in order to scale to the ZSE-18, 40:1 L:D ratio extruder. In this study, SME was used as the initial means of scaling, in order to ensure the dissolution of meloxicam in copovidone. The optimal SME for this system based on our prior work with the Nano-16 is 1.8 kW-h/kg. Based on the equation for SME [13],

$$\text{Specific energy (kW} \cdot \text{h/kg)} = \frac{\text{energy applied (kW)}}{\text{feed rate (kg/h)}} \quad (3)$$

$$\text{Energy applied (kW)} = \text{motor rating (kW)} * \text{torque (\%)} \quad (4)$$

$$* \frac{\text{screw speed}}{\text{maxscrew speed}} * \text{gearbox efficiency}$$

where the motor rating, max screw speed, and gearbox efficiency for the ZSE-18 were 3.9 kW, 500 rpm, and 0.97, respectively. Screw speed and feed rate are the primary variables that can be altered to vary SME; however, different combinations of parameters can achieve the same SME. In the first attempt, screw speed (200 rpm) was replicated and the temperature profile of zones 1–7 and the die (120–120–130–130–140–140–140 °C) was made to simulate zones 1–3 and the die of the Nano-16. Feed rate was adjusted to 0.41 kg/h to achieve 1.8 kW-h/kg SME on the Micro-18.

Additional optimization was performed. The degree of fill, which is described by Eq. 5, was increased.

$$\text{Degree of fill (\%)} = \frac{\text{feed rate} * K}{V * \frac{\text{screw speed}}{60 \text{ min}} * \text{SG} * \text{Screw efficiency}} * 100, \quad (5)$$

The feed rate is in kilograms per hour, *K* is a constant, *V* is the free volume in the extruder, *SG* is the specific gravity of the feed material, and screw efficiency relates to the forward-

conveying efficiency of the screw design [14]. The free volume in the Micro-18 extruder is $3.2 \text{ cm}^3/\text{m}$, the constant K is 0.277 g/s , SG was assumed to be 1 g/cm^3 , and the screw efficiency was assumed to be 0.175. This assumption was based on the aggressive screw design (>20% screw elements with low conveying efficiency versus <10% in the Nano-16 screw design). Screw speed and feed rate were varied with increased degree of fill. A list of the conditions is presented in Table I. The optimized screw design is presented in Fig. 1 and consists of three mixing zones. The first mixing zone contains moderate 30° and 60° kneading blocks, followed by a short more aggressive 90° kneading block, and finally three 90° kneading blocks in the final mixing zone. The barrel configuration consisted of two vents in zones 2 and 4, vacuum in zone 6, and a closed zone before the die.

Reduced Melt Residence Time

In order to achieve minimal residence time, downstream feeding of meloxicam was employed. Copovidone was introduced into the feed zone of the extruder by a gravimetric feeder at 0.54 kg/h , and the screw speed varied from 100 to 600 rpm in 100 rpm intervals. Meloxicam was introduced manually at the second vent in zone 4 (see Fig. 1), after which it went through a set of kneading elements and an additional vent before exiting the extruder. Residence time was measured with a previously reported method [15] using the presence of indigo carmine. Briefly, 1 g of indigo carmine was charged at the zone 2 vent along with meloxicam, and this was denoted as $t=0$. The extrudate exiting the die was monitored with a light and the residence time was denoted as the time when dye was first seen exiting the die.

Reduced Meloxicam Particle Size Study

A lab-scale Aljet air jet mill (model 00 Jet-O-Mizer, Fluid energy, Telford, PA) was used to micronize meloxicam to a particle size with a d_{90} of approximately $8 \mu\text{m}$. The grind pressure was set to 70 psi and the pusher nozzle to 50 psi. Meloxicam was fed into the mill at 5 g/min . The micronized meloxicam was then blended with copovidone as reported in “Melt Extrusion” and subsequently extruded with the optimal conditions from the scaling study presented in “Scale-Up.”.

Meloxicam-Meglumine Extrusion Study

For this study, 10% (w/w) or 20% (w/w) of meloxicam in the blend was maintained; however, a 1:1 M ratio of

meloxicam to meglumine was introduced by replacing the appropriate amount of copovidone with meglumine. The blend was prepared as described in “Melt Extrusion.”. All optimized process parameters with the exception of barrel temperature were used. The temperature profile utilized was 140, 140, 140, 140, 144, 144, and 144°C for zones 1–7 and the die, respectively.

In-line UV Spectroscopy to Monitor Degradation

In-line UV-VIS spectroscopy was performed during the extrusion runs. A transmission polymer melt probe (TPMP) (ColVisTec AG, Berlin, Germany) equipped with a 5-m fiber optic cable was used to take real-time spectral measurements from 220 to 820 nm. The probe was calibrated with a 5-mm gap and positioned at the exit of the extruder before the die. Blank measurements of PVPVA were also used to calibrate the probe. Spectral transmittance was used to monitor the undissolved meloxicam and increasing level of degradants in the extrudate. The data presented is a representative spectrum from the respective extrusion condition after reaching steady state.

Particle Size Analysis

The particle size distribution of the micronized meloxicam was analyzed using a HELOS laser diffraction instrument (Sympatec GmbH, Germany) using RODOS dispersion at 3 bar. Measurements were taken every 10 ms following powder dispersion. Measurements between 10 and 20% optical densities were averaged to determine the particle size distribution. An $n=3$ measurements was taken for the milled material and averaged.

Sample Preparation for Impurities Analysis

The milled and sieved extrudates were weighed and accurately transferred to volumetric flasks in triplicate to prepare $100 \mu\text{g/ml}$ solutions of meloxicam. A 50:50 volume ratio of methanol to 0.1 N NaOH mixture was used as the diluent. A small volume of diluent was added to the volumetric flask and sonicated for 5 min before filling to volume. The solutions were then filtered through $0.22 \mu\text{m}$, 13-mm PTFE filters (Whatman, Pittsburgh, PA) and immediately transferred to 2-ml HPLC vials for analysis.

HPLC Analysis

Meloxicam and any degradant content were analyzed with a Thermo Scientific Dionex UltiMate 3000 HPLC System (Thermo Scientific, Sunnyvale, CA, USA). An Ultimate 3000 Autosampler was utilized to inject $20\text{-}\mu\text{l}$ samples. The HPLC system also included dual UltiMate Pumps and an UltiMate RS Variable Wavelength Detector operating at 254 nm. The aqueous mobile phase (MP) consisted of 0.1% (v/v) phosphoric acid while the organic phase consisted of acetonitrile. A gradient that operated at 0.8 ml/min ran from 5% organic MP to 95% organic MP over 15 min separated impurities. Injections were passed through a Waters SunFire™ C18 reverse phase column, $4.6 \text{ mm} \times 150 \text{ mm}$, with $4.6 \mu\text{m}$ packing (Waters Corporation, Milford,

Table I. Extruder Conditions for the Nano-16 and Micro-18 with the Same Specific Mechanical Energy Input for Initial Scale-Up

Extruder conditions	ZSE-18	Nano-16
Screw speed	200 rpm	200 rpm
Feed rate	0.41 kg/h	0.24 kg/h
Barrel temperature ($^\circ\text{C}$)	120–120–130–130–130–140–140–140	110–110–140–140
Degree of fill	6.1%	6.3%
SME	1.8 kW-h/kg	1.8 kW-h/kg

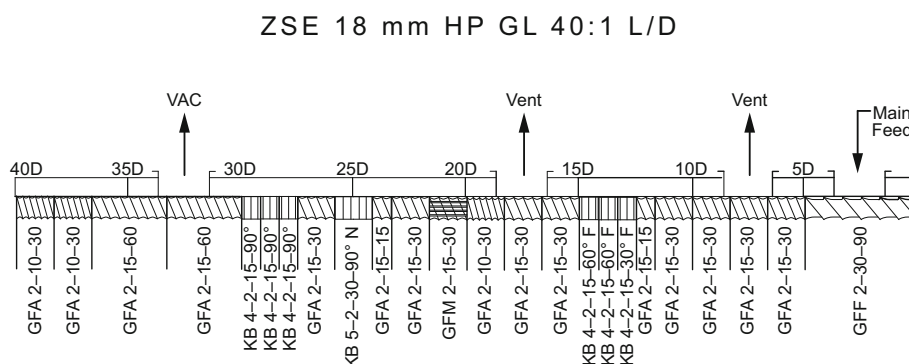


Fig. 1. Optimized barrel configuration and screw design with venting and vacuum to remove moisture and three mixing sections to fully convert meloxicam to its amorphous form

MA, USA) kept at room temperature. The retention time of meloxicam was approximately 12.8 min. Purity was reported as an average of the percentage peak area of meloxicam with respect to all impurity peaks. All analyses maintained linearity in the range tested. Chromeleon Version 6.80 software (Thermo Scientific, Sunnyvale, CA, USA) was used to process all chromatography data.

Powder X-ray Diffraction

Powder X-ray diffraction (PXRD) analyses were conducted on a Rigaku Miniflex600 (Rigaku Americas, The Woodlands, Texas, USA) instrument equipped with a Cu-K α radiation source generated at 40 kV and 15 mA. Samples were scanned in continuous mode with a step size of 0.02° over a 2θ range of 10–40° at a rate of 1°/min¹. No significant diffraction peaks were seen below 10° 2θ or above 40° 2θ for the materials during the initial screening. Data were compiled using Microsoft Excel and plotted in GraphPad Prism 6 software (GraphPad Software Inc., La Jolla, CA).

Polarized Light Microscopy

Trace crystalline meloxicam was evaluated with polarized light microscopy (PLM). Milled extrudate was dusted onto a glass slide with a drop of mineral oil and covered with a glass coverslip. Analyses were conducted on an Olympus BX-53 (Olympus, Waltham, MA) polarizing light microscope with a first-order red compensator at $\times 200$ magnification. To detect any light refractions, the stage was rotated at least 90° while observing each sample. Images were taken with a QICAM digital camera (QImaging, BC, Canada) with Qcapture, v 2.0.13 (QImaging, BC, Canada).

RESULTS AND DISCUSSION

Optimizing SME Input for Larger Extruder with Different Geometries

Differences in screw geometry will have a major impact on the scale-up of the process from the Nano-16 to the ZSE-18 [5]. The Nano-16 was designed for early development, therefore, it has a low free volume of 0.9 cm³/diameter which minimizes the material required for each run. The different

screw geometries of the Nano-16 and ZSE-18 are presented in Fig. 2. For the Nano-16, the clearance between the barrel wall and the outer diameter of the screws is small and the screws are trilobal resulting in high shear along the barrel wall. The ZSE-18 extruder has a free volume of 3.2 cm³/diameter, which is more than double the Nano-16. The screw geometry is bilobal allowing for less shear. The difference in peak shear between the two geometries is also depicted in the diagram in Fig. 2. The trilobal screw geometry allows for three places of high shear (indicated in red) whereas the bilobal screw geometry only has two (also indicated in red). Additionally, the bilobal screws have a larger pitch or deeper

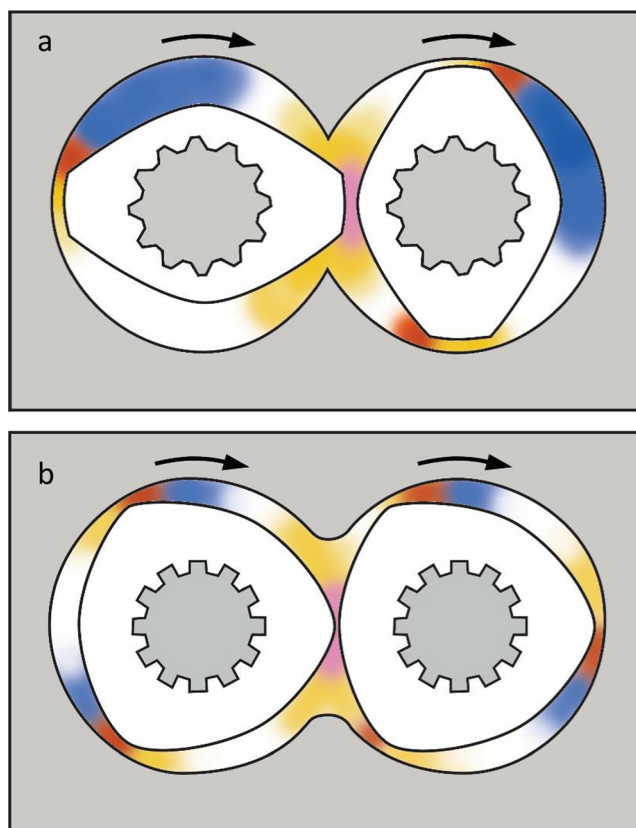


Fig. 2. Cross-sectional view of different screw geometries: **a** bilobal TSE screw elements and **b** trilobal TSE screw elements

threading which reduces the surface area of material pressed against the barrel wall. The other impact that the low free volume has on the extrusion process is the temperature control. Materials in the Nano-16 will be impacted by the barrel temperature more than in the ZSE-18 because of the larger surface area in contact with the barrel wall [3]. Due to the larger L:D ratio, 40:1 versus 25:1, and consequential mixing rotations, the energy generated by the screws play a more significant role on the melt temperature in the ZSE-18. Evidence of this is indicated in the temperature profiles for the Nano-16 and ZSE-18 (Table I). Due to the smaller free volume and greater heat exchange from the barrels in the Nano-16, the temperature profile is lower prior to the kneading elements and melting of meloxicam. The ZSE-18 had a slightly higher temperature profile because heat wasn't transferred as efficiently from the barrels and also to accommodate the increase in torque from the higher feed rate in the zones before meloxicam was melted.

Our initial attempt to scale-up the process was to use SME, which incorporates all four major extrusion processing parameters (feed rate, screw speed, barrel temperature, and barrel configuration/screw design). Feed rate and screw speed are directly related (Eqs. 3 and 4) while the other two parameters are built into the % torque term of the expression. To indicate the importance of factoring in the screw geometry difference as well as SME, screw geometry was initially ignored and the conditions of the Nano-16 were replicated as closely as possible. Both conditions are presented in Table I for reference. The resultant materials were brown and bubbly indicating significant degradation. Fortunately, similar SME can be achieved with a different combination of processing parameters so that it can be scaled to accommodate for geometry differences between the Nano-16 and ZSE-18 extruders.

The optimized barrel configuration is presented in Fig. 1. The scaled process also incorporated vacuum to remove moisture, as our previous work showed that meloxicam degrades by hydrolysis during extrusion [11]. Despite pre-drying the polymer before extrusion, some moisture remained. Implementing vacuum into the process required seals in the screw design to effectively create a vacuum pull. Initially, this was a concern due to high shear in the seals that could lead to degradation. However, based on the lower peak shear in the ZSE-18, an aggressive screw design was necessary for complete amorphous conversion. The temperature profile of zones 1–7 and the die were 122, 122, 133, 133, 144, 144, 155, and 155 °C, respectively, which achieved a melt temperature of approximately 151 °C. At barrel temperatures higher than these, significant degradation was observed as indicated by dark brown and bubbly extrudate, and high torque was observed below these temperatures which exceeded the limit of the gearbox preventing extrusion.

Next, the final two processing parameters, screw speed and feed rate, were optimized. The equation for feed rate when scaling between different screw geometries, Eq. 2, was used to calculate an approximate scaled feed rate (2.6 kg/h). This equation assumes the L:D ratio is the same, so it was used to identify a processing window not an exact feed rate. From this approximate feed rate, screw speeds were chosen that provided a SME within a window (1.2–1.8 kW-h/kg) of the optimized SME of 1.8 kW-h/kg. The conditions tried and results are presented in Table II.








None of the attempted conditions achieved 100% purity of meloxicam. Additionally, none of the ASDs had complete amorphous conversion unless they experienced significant degradation (batches 1 and 2). Based on the dark brown extrudate, SME was reduced between batches 2 and 3 by increasing feed rate. Batch 3 was greatly improved as indicated by its purity which is 91.6% up from 79.2% of batch 2. However, the extrudate remained darker than the optimized material from the Nano-16. Screw speed was reduced to 333 rpm to further reduce the SME. The feed rate was set to 1.8 kg/h. The extrudate had improved purity of 94.5% however was opaque. The degree of fill under these conditions, 16.1%, was not enough to ensure efficient mixing. Feed rate was increased back to 2.0 kg/h. This extrudate appeared yellow and translucent. Increasing the feed rate for batch 5 with all other conditions held constant from batch 4, SME is reduced and the expectation is that degradation would also decrease. However, purity decreased from 94.5 to 92.7%. The purity of Batch 4 is high because the amorphous conversion was not as efficient due to the low degree of fill in the screws. Batch 5 conditions were the best and therefore used to investigate the impact of vacuum. Batch 6 was processed using the optimized conditions of batch 5 without a vacuum pull. There is a small difference in the purity. Despite the lack of vacuum, batch 6 still had a significant amount of venting and polymer was pre-dried. We expect the difference in the results to be larger if there was less venting and if polymer was not dried before extrusion. However, running an experiment like this is challenging. We attempted it in our previous study [11], but residual moisture in the system also plasticized the system and did not allow for good amorphous conversion.

Though batch 5 was optimal from this study, crystalline material, not visible to the eye, was detected by PXRD (Fig. 3) in the formulation. This small crystalline peak in the diffraction pattern was verified by PLM (data not shown).

Reduced Melt Residence Time by Downstream Feeding Study

Reducing the melt residence time and thermal exposure of drug substances in the extruder has been successful in the past [15, 16]. Reduced melt residence time was attempted because none of the initial scaled processing conditions resulted in 100% purity of meloxicam and because it had improved purity on the Nano-16. In order to achieve a short melt residence time on the Nano-16, the temperature was kept well below the suppressed melting point of meloxicam until the last zone where the temperature was increased and a set kneading blocks were put to ensure amorphous conversion. This technique could not be achieved with the ZSE-18 due to torque constraints and the longer L:D ratio. Reduced melt residence time could be achieved on the ZSE-18 by increasing feed rate and screw speed or by downstream feeding. Downstream feeding afforded two advantages; (1) reduced melt residence time and (2) removal of moisture before meloxicam exposure to copovidone. Based on this added advantage, downstream feeding was chosen as the strategy for reducing melt residence time. Copovidone was introduced in the feeding zone and meloxicam was added downstream at the second vent. This reduced the melt residence time from 3 to 5 min down to <30 s. However, the results were not as expected. Amorphous conversion of

Table II. Extrusion Processing Conditions, Extrudate Appearance, and Percentage Purity After Extrusion

Batch	Condition	Degree of Fill (%)	Feed Rate (kg/hr)	Screw Speed (rpm)	Barrel Temp. (°C)	Avg. Purity (%)	Visual	XRD
1	10% MLX	3.3	0.5	450	122-122-133-133-144-144-155	75.5±0.76%		Amorphous
2	10% MLX	3.7	0.5	400	122-122-133-133-144-144-155	79.2±0.57%		Amorphous
3	10% MLX	14.9	2.0	400	122-122-133-133-144-144-155	91.6±0.75%		Semi-crystalline
4	10% MLX	16.1	1.8	333	122-122-133-133-144-144-155	94.5±0.40%		Semi-crystalline
5	10% MLX optimized	17.9	2.0	333	122-122-133-133-144-144-155	92.7±0.06%		Semi-crystalline
6	10% MLX no vac.	17.9	2.0	333	122-122-133-133-144-144-155	91.4±0.80%		Semi-crystalline
7	Jet milled	17.9	2.0	333	122-122-133-133-144-144-155	97.2±0.06%		Amorphous

meloxicam could not be achieved at the low residence times; the extrudates from the downstream feeding were opaque. In order to improve the conversion, barrel temperatures as high as 190 °C, and screw speeds as high as 600 rpm were employed. However, the extrudate remained opaque with visible residual crystalline meloxicam.

While these results were not expected, they illustrate the mechanism behind the mixing of meloxicam and copovidone in the extruder. Because the extruder is operated at a temperature below the melting point of meloxicam, the process of forming an ASD is a dissolution process rather than liquid-liquid mixing. Therefore, the process requires time in order for meloxicam to fully dissolve in copovidone. In this case, the minimal melt residence time is not optimal.

Reduced Meloxicam Particle Size Study

Due to the persisting degradants from the initial scale-up work and the residual crystalline meloxicam from the

downstream feeding experiment, we hypothesized that increasing the dissolution rate of meloxicam in copovidone would be advantageous. Reducing the time for the amorphous conversion would improve the results both by allowing for a reduced melt residence time for reduced degradation and by decreasing the amount of energy required for amorphous conversion of meloxicam. Dissolution can be described by the Noyes-Whitney Equation [17];

$$\text{Dissolution rate} = A \frac{D}{d} (C_s - C_b) \quad (4)$$

where A is the surface area of the material, D is the diffusion coefficient, d is the thickness of the boundary layer, and C_s and C_b are the concentration of the substance at the surface and in the bulk, respectively. In this expression D , C_s , and C_b are fixed, so in order to increase the dissolution rate, either the boundary layer thickness needs to be reduced or the surface area needs to be increased. In this case, the easiest

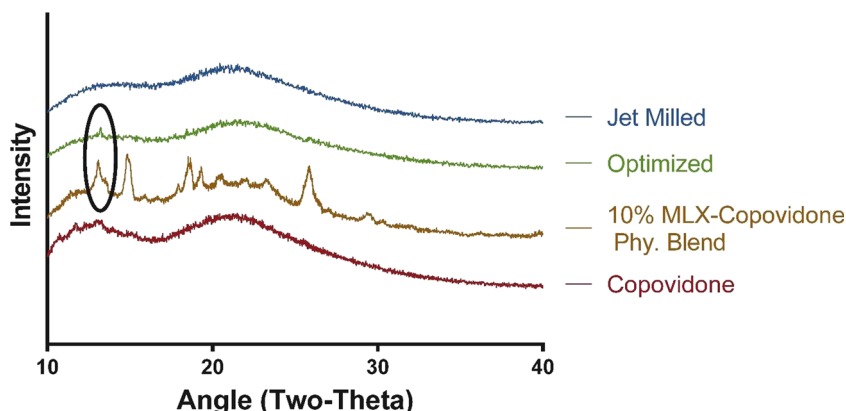


Fig. 3. PXRD diffractograms of copovidone, 10% meloxicam-copovidone physical blend, extrudate from the optimized conditions, and the extrudate from jet milled meloxicam with optimized conditions. The optimized condition extrudate has a crystalline peak, indicated by the black circle, while the jet-milled extrudate is completely amorphous

way to increase the dissolution rate was to increase the surface area by reducing the particle size of meloxicam. Meloxicam was micronized down to a d_{90} of 8 μm from an initial d_{90} of 40 μm using a jet mill and subsequently extruded with the optimized parameters from the scale-up study. The conditions and resultant extrudate from this run are presented in Table II, batch 7. The purity level of the material was increased to 97.2% which is the optimal level of purity which was achieved on the Nano-16. Additionally, with the processing conditions held constant, more meloxicam was able to dissolve. The jet milled extrudate was amorphous by PXRD (Fig. 3) and PLM (Fig. 4).

In-line UV-VIS Spectroscopy for Extrudate Quality Monitoring in Real Time

In-line monitoring was applied during scale-up to facilitate optimizing the process in real time. Advantages of optimizing with in-line monitoring include no sampling, no material loss, and real-time adjustments for efficient optimization [18]. In-line monitoring has previously been implemented during extrusion with the use of near-infrared (NIR) and Fourier transform infrared (FTIR) probes [19, 20]. While these techniques have been used, they also have limitations including spectral overlap of functional groups from drug substances and polymer that can make quantitative measurements complicated [21]. In particular, polymer carriers tend to have large broad absorption bands that can mask bands attributed to drug substances. As an alternative, in-line UV-VIS spectroscopy can be implemented. It has been applied previously in the plastic industry to monitor degradation of polymers [22, 23].

The UV-VIS, fiber optic probe employed in this study is capable of measuring translucent molten materials. Typically, drug substances will show broad but distinct absorption in the UV range due to the resonance of their aromatic structures. In addition, light scattering will take place when features (such as crystalline particles), with a refractive index different from the refractive index of the polymer carrier are present. Depending on the size of these particles, scattering can be wavelength dependent ($\text{size} \leq \text{wavelength}$) or constant over the entire wavelength range ($\text{size} \gg \text{wavelength}$). Typically, drug substances have particle sizes in the micron range, and therefore have constant scatter across wavelengths.

Light scattering will lead to a substantial drop (order of magnitude) in the light level transmitted even for trace amounts of particles. An example of the scattering and correspondent

drop in transmittance from undissolved meloxicam (incomplete amorphous conversion) is presented in Fig. 5, batch 5 (optimized extrusion conditions). Recall that batch 5 appeared visually translucent and residual crystalline meloxicam was only detected by PXRD. In comparison, there is no loss in transmittance in the spectrum in Fig. 5 from batch 7. This extrudate was prepared under the same optimized conditions however with jet milled meloxicam. These results are consistent with the PXRD (Fig. 3) results where crystalline (undissolved meloxicam) was detected in the batch 5 extrudate but not in batch 7 extrudate. The in-line probe allowed for detection of undissolved meloxicam that was not detectable by visual observation alone and required post-processing analysis. These results demonstrate the advantage of using in-line UV-VIS monitoring.

Additionally, the in-line UV-VIS monitoring allowed us to track the relative level of degradation between extrusion conditions. The shape of the band in the spectrum is broadened with further extension into the visible range as the level of degradant increased. An example of the phenomenon we observed is shown in Fig. 5, batches 1 and 7. Both impurities, generated by hydrolysis during extrusion (refer to ref. [24]), have strong absorption in the UV range at ~ 260 nm whereas meloxicam itself has a strong absorption at 360 nm, closer to the visible range. Based on this information, we would expect a stronger absorption in lower wavelengths as degradation is increased. Instead, the broadening of the absorption band into the visible range, not UV range, is likely related to the color of the extrudate. Meloxicam extrudate, which has little impurities, is clear and yellow in color. Alternatively, when a high level of impurities are present, it appears dark brown. Brown wavelengths are lower frequency, and are consistent with the broadening to larger wavelengths in the visible area. This broadening into the visible range was also observed during in-line UV monitoring of the degradation of poly(L-lactic acid) [25]. Wang *et al.* found that in-line UV-VIS spectroscopy is highly sensitive to color changes which correlated well with degradation of poly(L-lactic acid). In order to apply in-line UV-VIS monitoring as a quantitative technique for our model system, further characterization of the spectra of both the pure and degraded extrudate is necessary.

From these observations, the extrusion could be altered to improve the results in real time without having to sample, analyze the extrudate, and adjust the extrusion conditions. While the UV-VIS monitoring was exploratory in this study, the method could be used quantitatively in future studies both for amorphous conversion and level of degradation.

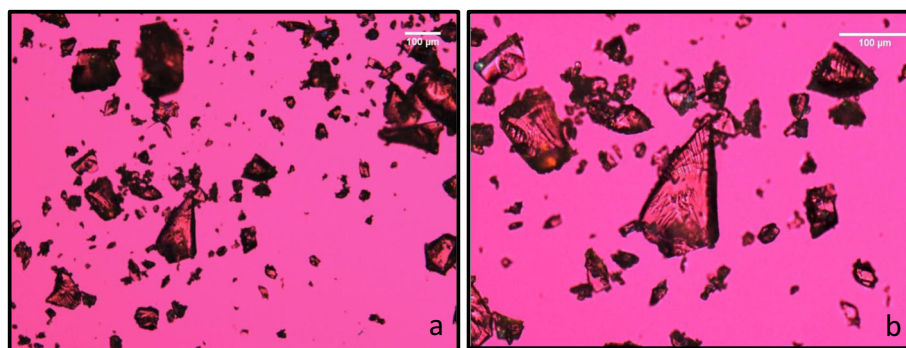


Fig. 4. PLM images of the extrudate prepared from jet milled meloxicam at **a** $\times 100$ and **b** $\times 200$ magnifications

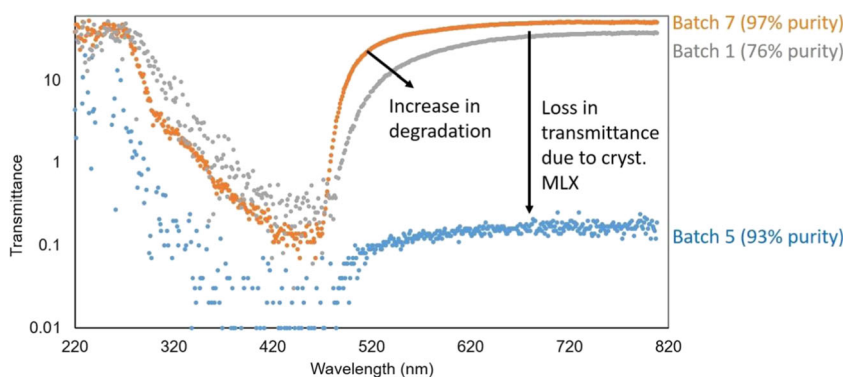


Fig. 5. In-line UV-VIS transmittance from scaled-up extruder conditions of batches 1, 5, and 7

Meloxicam-Meglumine Extrusion Study

Despite advantages of scaling from the Nano-16 to the ZSE-18 extruder, the purity of meloxicam could not be improved upon from the Nano-16 process. Additional unit operations such as vacuum, downstream feeding, and additional screw configurations due to the 40:1 L:D ratio, were all only able to achieve the same purity level (~97%) that was achieved in the Nano-16. These additional unit operations and the reduced shear associated with the bilobal screw geometry were not sufficient for full amorphous conversion. As was observed on the Nano-16, when processing conditions alone were not sufficient, a formulation adjustment can be made to achieve 100% purity [26].

Addition of Meglumine for 100% Purity

We previously showed that meglumine improves the purity after extrusion on a Nano-16 extruder in a meloxicam-copovidone ASD [11]. The presence of meglumine in the extruder ionizes meloxicam so that it can form an ionic interaction (*in situ* salt formation) with meglumine. This interaction disrupts the hydrolysis of meloxicam. Meglumine was added in a 1:1 M ratio to meloxicam which was identified as the ideal molar ratio and extruded on the ZSE-18 with the optimized conditions with the exception of barrel temperature which was increased due to increased torque. The new temperature profile was 140, 140, 140, 140, 144, 144, 144, and

144 °C for zones 1–7 and the die, respectively. The increase in torque can be explained by anti-plasticization from the strong ionic interaction between meloxicam and meglumine. Despite the fact that the melting point of meloxicam is further suppressed in the presence of meglumine to a temperature of 110 °C [11], the processing temperature required is actually higher. This behavior has been observed before [27–29]. Mistry et al. measured the molecular mobility of ketoconazole with three polymers where ketoconazole exhibited different interactions including ionic, hydrogen bonding, and dipole interactions [29]. They concluded that molecular mobility was most reduced with the strong ionic interaction.

The results from the extrusion run with meglumine are presented in Table III (batches 8 and 9). In comparison with the extrudate without meglumine, it was slightly darker, but appeared translucent and yellow. When processed with meglumine, there is complete amorphous conversion and 100% purity. Therefore, the formulation modification used for small-scale production was also successful for extruding on the larger scale.

Addition of Meglumine for Increased Drug Loading

Amorphous conversion of meloxicam was difficult on the ZSE-18 extruder. Reducing particle size of the material enhanced the conversion but did not allow for full conversion. The meloxicam-meglumine-copovidone ASD had full conversion with little difficulty. Based on this, we believed that meglumine was not only stabilizing meloxicam but could also

Table III. Processing Conditions and Results from Batches with 10 and 20% Meloxicam with and without Meglumine

Batch	Condition	Feed Rate (kg/hr)	Screw Speed (rpm)	Barrel Temp. (°C)	Avg. Purity (%)	Visual	Complete amorphous conversion?
8	10% MLX optimized	2.0	333	122-122-133-133-144-144-155	92.7±0.37%		Almost by XRD
9	10% MLX MGL	2.0	333	140-140-140-144-144-144-144	100.0±0.0%		Yes
10	20% MLX	2.0	333	122-122-133-133-144-144-155	94.5±0.40%		No
11	20% MLX MGL	2.0	333	140-140-140-144-144-144-144	100.0±0.0%		Almost by XRD

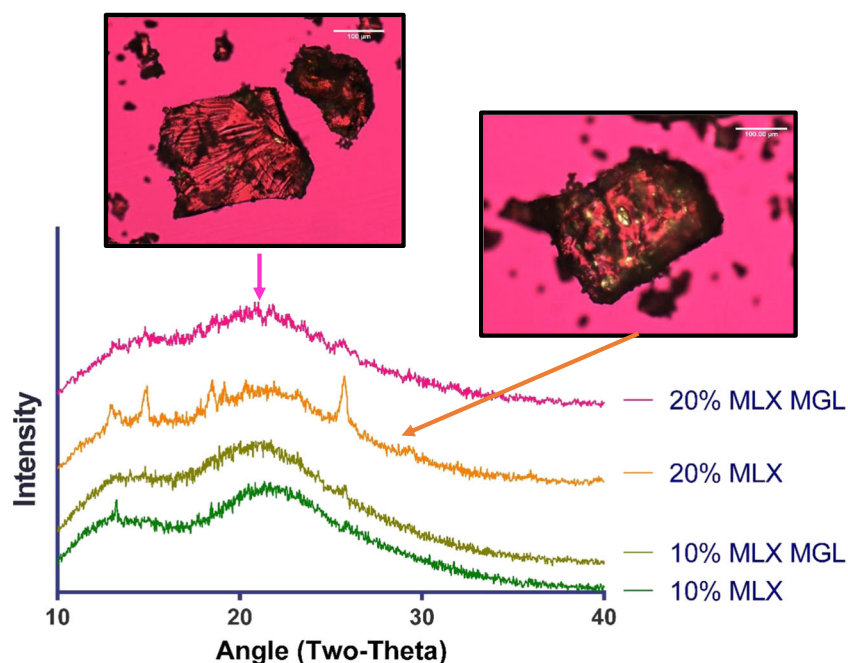


Fig. 6. PXRD diffractograms of the 10 and 20% meloxicam (MLX) extrudate, as well as the extrudates which contain meglumine (MGL). PLM images of the 20% MLX extrudate and 20% MLX MGL extrudate are also shown

improve the solubility of meloxicam in copovidone. As a result, increased meloxicam loading was extruded with and without meglumine for comparison. The 1:1 M ratio of meloxicam to meglumine was maintained. The results are presented in Table III (batches 10 and 11). The increased meloxicam loading (20%) formulation with meglumine (batch 11) had 100% purity and was mostly amorphous by PXRD (Fig. 6). The control, without meglumine (batch 10), had similar purity as the 10% meloxicam loading; however, the extrudate had low amorphous conversion. It had an opaque

appearance (Table III, batch 10) and contained a lot of residual crystalline meloxicam by PXRD and PLM (Fig. 6). These results verify the added solubility advantage of meglumine. Meloxicam has pH-dependent solubility and is more soluble in basic pH. Copovidone has a slightly acidic pH (4–7) [30] due to cleavage of acetyl groups during manufacturing. The presence of meglumine increases the pH of the system and therefore increases the solubility. Additionally, meglumine further suppresses the melting point of meloxicam from ~175 °C in the presence of copovidone to

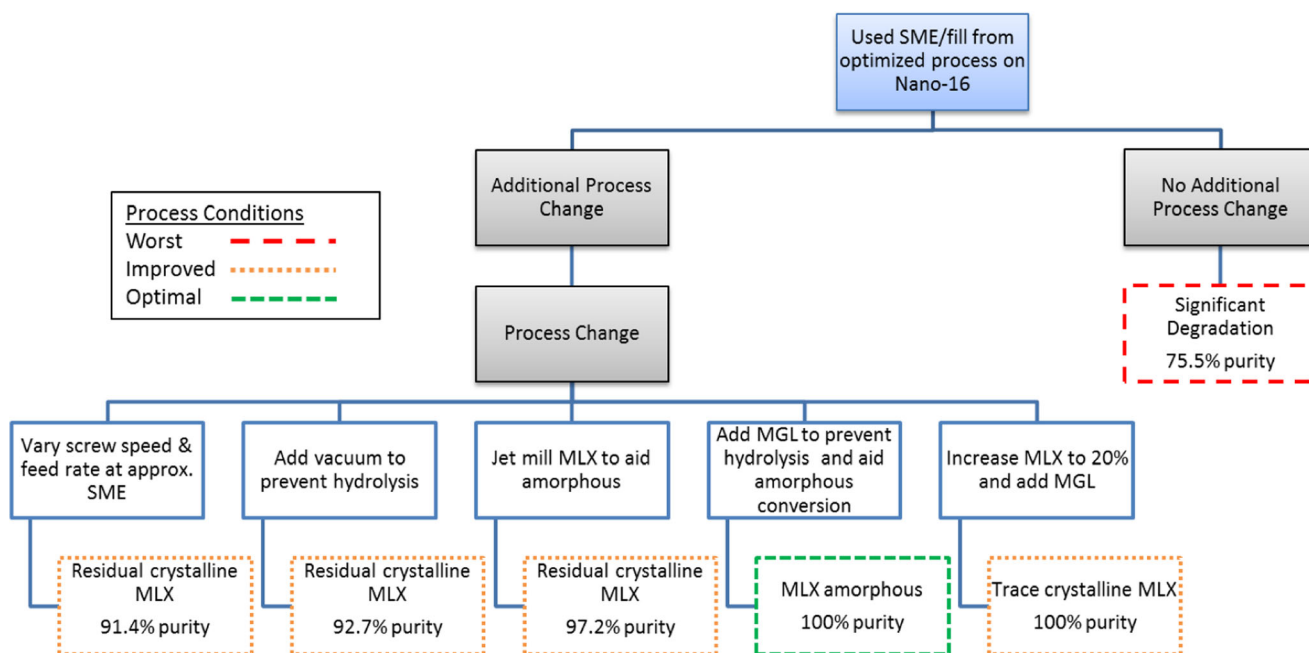


Fig. 7. Schematic of the process optimization done in order to scale the process from the Nano-16 to the ZSE-18

110 °C [11]. This drop in temperature should allow for more liquid-liquid mixing of meloxicam reducing the energy and time required for full amorphous conversion.

CONCLUSIONS

While larger-scale extrusion equipment offers additional flexibility in terms of screw design, unit operations, and residence time as well as reduced peak shear when going from a trilobal to bilobal screw geometry, the impact on chemical degradation of drug substances is complex. We were unable to improve the purity after extrusion of meloxicam from the Nano-16 to the ZSE-18. Instead, important findings regarding the scaling between dissimilar geometries and the mechanism of formation were reported. Barrel temperature, specific mechanical energy input, and degree of fill were all critical to scaling the process. Due to the reduced peak shear of the bilobal geometry, full amorphous conversion of meloxicam was a challenge. A more aggressive screw design was employed in addition to micronized meloxicam which reduced the time and energy required to convert meloxicam. Meglumine was added to the formulation to stabilize meloxicam when process conditions alone were not sufficient. In addition to stabilizing meloxicam it also improved the solubility of meloxicam allowing for increased drug loading. A schematic that summarizes the process optimization is presented in Fig. 7. We demonstrated that scale-up of an extrusion process across dissimilar geometries can be achieved and that findings from small-scale equipment are indicative of larger scale findings.

ACKNOWLEDGEMENTS

Some of this work was presented at the 2017 AAPS Annual Meeting and Exhibition, San Diego, CA. The authors would like to acknowledge Nada Kittikunakoin for her help in completing this work.

REFERENCES

- Repka MA, Majumdar S, Kumar Battu S, Srirangam R, Upadhye SB. Applications of hot-melt extrusion for drug delivery. *Expert Opin Drug Deliv*. 2008;5(12):1357-76.
- LaFountaine JS, McGinity JW, Williams RO. Challenges and strategies in thermal processing of amorphous solid dispersions: a review. *AAPS PharmSciTech*. 2016;17(1):43-55.
- Brown C, DiNunzio J, Eglesia M, Forster S, Lamm M, Lowinger M, Marsac P, McKelvey C, Meyer R, Schenck L, Terife G. Hot-melt extrusion for solid dispersions: composition and design considerations. In: *Amorphous solid dispersions*. New York: Springer; 2014. p. 197-230.
- Brown C, DiNunzio J, Eglesia M, Forster S, Lamm M, Lowinger M, Marsac P, McKelvey C, Meyer R, Schenck L, Terife G. HME for solid dispersions: scale-up and late-stage development. In: *Amorphous solid dispersions*. New York: Springer; 2014. p. 231-260.
- Dreiblatt A. Technological considerations related to scale-up of hot-melt extrusion processes. In: Douroumis D, editor. *Hot-melt extrusion: pharmaceutical applications*. 1st ed. UK: John Wiley & Sons, Ltd; 2012. p. 285-300.
- Carley JF, McKelvey JM. Extruder scale-up theory and experiments. *Ind Eng Chem*. 1953;45(5):989-92. <https://doi.org/10.1021/ie50521a036>.
- Tadmor Z, Gogos CG. *Principles of polymer processing*. 2nd ed. UK: John Wiley & Sons; 2013.
- Booy M. Influence of channel curvature on flow, pressure distribution, and power requirements of screw pumps and melt extruders. *Polym Eng Sci*. 1963;3(3):176-85.
- Agrawal AM, Dudhedia MS, Zimny E. Hot melt extrusion: development of an amorphous solid dispersion for an insoluble drug from mini-scale to clinical scale. *AAPS PharmSciTech*. 2016;17(1):133-47. <https://doi.org/10.1208/s12249-015-0425-7>.
- Nakatani M. Scale-up theory for twin-screw extruder, keeping the resin temperature unchanged. *Adv Polym Technol*. 1998;17(1):19-22.
- Haser A, Huang S, Listro T, White D, Zhang F. An approach for chemical stability during melt extrusion of a drug substance with a high melting point. *Int J Pharm*. 2017;524(1):55-64.
- Todd DB. *Plastics compounding: equipment and processing*. Munich: Carl Hanser Verlag GmbH & Co; 1998.
- Martin C. Twin screw extruders as continuous mixers for thermal processing: a technical and historical perspective. *AAPS PharmSciTech*. 2016;17(1):3-19. <https://doi.org/10.1208/s12249-016-0485-3>.
- Martin C. Twin screw extrusion for pharmaceutical processes. In: *Melt extrusion*. New York: Springer; 2013. p. 47-79.
- Keen JM, Martin C, Machado A, Sandhu H, McGinity JW, DiNunzio JC. Investigation of process temperature and screw speed on properties of a pharmaceutical solid dispersion using corotating and counter-rotating twin-screw extruders. *J Pharm Pharmacol*. 2014;66(2):204-17.
- Huang S, O'Donnell KP, de Vaux SMD, et al. Processing thermally labile drugs by hot-melt extrusion: the lesson with Gliclazide. *Eur J Pharm Biopharm*. 2017;119:56-67.
- Martin AN, Swarbrick J, Cammarata A. *Physical pharmacy: physical chemical principles in the pharmaceutical sciences*. 3rd ed. Philadelphia: Lea & Febiger; 1993.
- Saerens L, Vervaeke C, Remon JP, de Beer T. Process monitoring and visualization solutions for hot-melt extrusion: a review. *J Pharm Pharmacol*. 2014;66(2):180-203.
- Almeida A, Saerens L, De Beer T, et al. Upscaling and in-line process monitoring via spectroscopic techniques of ethylene vinyl acetate hot-melt extruded formulations. *Int J Pharma*. 2012;439(1):223-9. <https://doi.org/10.1016/j.ijpharm.2012.09.037>.
- De Beer T, Burggraef A, Fonteyne M, et al. Near infrared and Raman spectroscopy for the in-process monitoring of pharmaceutical production processes. *Int J Pharm*. 2011;417(1):32-47.
- Ingo A, Bernd S, Dirk L. Monitoring of polymer melt processing. *Meas Sci Technol*. 2010;21(6):062001.
- Kesters E, Vanderzande D, Lutsen L, Penxten H, Carleer R. Study of the thermal elimination and degradation processes of n-alkylsulfanyl-PPV and -OC1C10-PPV precursor polymers with in situ spectroscopic techniques. *Macromolecules*. 2005;38(4):1141-7.
- Malinauskas A, Holze R. In situ UV-vis spectroelectrochemical study of polyaniline degradation. *J Appl Polym Sci*. 1999;73(2):287-94.
- Haser A, Huang S, Listro T, et al. An approach for chemical stability during melt extrusion of a drug substance with a high melting point. *Int J Pharm*. 2017;524(1-2):55-64.
- Wang Y, Steinhoff B, Brinkmann C, et al. In-line monitoring of the thermal degradation of poly(l-lactic acid) during melt extrusion by UV-vis spectroscopy. *Polymer*. 2008;49(5):1257-65. <https://doi.org/10.1016/j.polymer.2008.01.010>.
- Haser A, Cao T, Lubach J, et al. In situ salt formation for improved chemical stability and dissolution performance of a meloxicam-copovidone amorphous solid dispersion. *Mol Pharm*. 2018;15(3):1226-37.
- Gupta P, Bansal AK. Modeling of drug release from celecoxib-PVP-meglumine amorphous systems. *PDA J Pharm Sci Technol*. 2005;59(6):346-54.
- Telang C, Mujumdar S, Mathew M. Improved physical stability of amorphous state through acid base interactions. *J Pharm Sci*. 2009;98(6):2149-59.
- Mistry P, Mohapatra S, Gopinath T, et al. Role of the strength of drug-polymer interactions on the molecular mobility and crystallization inhibition in ketoconazole solid dispersions. *Mol Pharm*. 2015;12(9):3339-50. <https://doi.org/10.1021/acs.molpharmaceut.5b00333>.
- Kolter K, Karl M, Gryczke A. Hot-melt extrusion with BASF pharma polymers. Ludwigshafen: BASF SE, Pharma Ingredients & Services; 2012.